

Advances in resistive wall mode stabilization to maintain high beta, low internal inductance plasmas in NSTX*

S.A. Sabbagh¹, J.W. Berkery¹, J.M. Bialek¹, S.P. Gerhardt², O. Katsuro-Hopkins¹, Y.S. Park¹, R.E. Bell², R. Betti², A. Diallo², D.A. Gates², B.P. LeBlanc², J.E. Menard², M. Podesta², K. Tritz³, H. Yuh⁴

¹Dept. of Applied Physics and Applied Mathematics, Columbia U., New York, NY, USA

²Princeton Plasma Physics Laboratory, Princeton U., Princeton, NJ, USA

³Johns Hopkins University, Baltimore, MD, USA

⁴Nova Photonics, Princeton, NJ, USA

Spherical torus (ST) fusion applications (e.g. a component test facility [1], or pilot power plant [2]) and steady-state advanced tokamaks aim to operate continuously at high normalized beta, $\beta_N \equiv 10^8 \langle \beta_t \rangle a B_0 / I_p$, ($\beta_t \equiv 2\mu_0 \langle p \rangle / B_0^2$) and high non-inductive current fraction. High bootstrap current fraction yields a broad current profile, equating to low plasma internal inductance, l_i . While low l_i operation is favourable for efficient non-inductive operation, it is generally unfavourable for global MHD mode stability, reducing the ideal $n = 1$ no-wall beta limit, $\beta_N^{no-wall}$. Operation of the National Spherical Torus Experiment (NSTX) has demonstrated high β_N operation with l_i typically in the range $0.6 < l_i < 0.8$, with $\beta_N^{no-wall}$ computed by the DCON code to be 4.2 – 4.4. [3] NSTX has more recently demonstrated transient $\beta_N > 6.5$ and $\beta_N/l_i > 13.5$, and pulse-averaged β_N (averaged over constant plasma

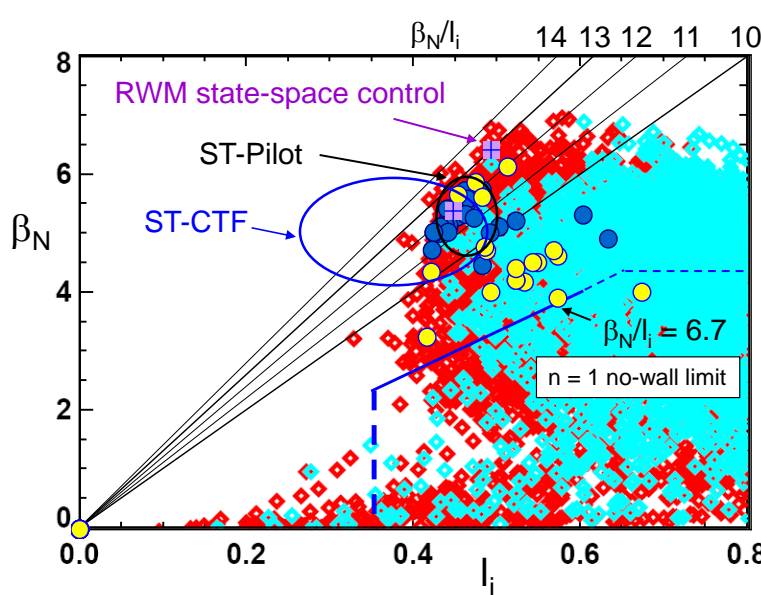


Fig. 1: High β_N attained at low l_i in NSTX appropriate for future ST devices. Red/cyan points indicate plasmas with/without $n=1$ active RWM control. Blue circles indicate stable long pulse plasma with active RWM control; yellow indicates disruptions.

current), $\langle \beta_N \rangle_{pulse} > 5.5$ in low l_i plasmas in the range $0.4 < l_i < 0.6$ with active $n = 1$ mode control (Fig. 1). Pulse-averaged values of (l_i, β_N) now intercept the higher l_i portion of the planned operational ranges for ST-CTF and ST Pilot plants. Especially important is that the ideal $n = 1$ no-wall stability limit is significantly reduced at these low l_i values, so that β_N now exceeds the DCON computed $\beta_N^{no-wall}$ for

equilibrium reconstructions of these plasmas by up to a factor of two. In addition, synthetic variations of the pressure profile for plasmas with $l_i \sim 0.38$ show these equilibria to be at the purely current-driven ideal kink stability limit, as they are computed to be ideal unstable at all values of $\beta_N > 0$. In this operational regime, passive or active kink and resistive wall mode (RWM) stabilization is therefore critical. Two new control approaches are investigated in NSTX. First, combined use of radial and poloidal field RWM sensors in proportional gain control provided feedback on $n = 1$ modes. The disruption probability due to unstable RWMs was reduced from 48% in initial low l_i experiments to 14% with this control, but remarkably, the reduced disruption probability was observed mostly in plasmas at high $\beta_N/l_i > 11$ (Fig. 1). Disruptions occurred more frequently at lower β_N . This behavior is examined in Fig. 2 for low

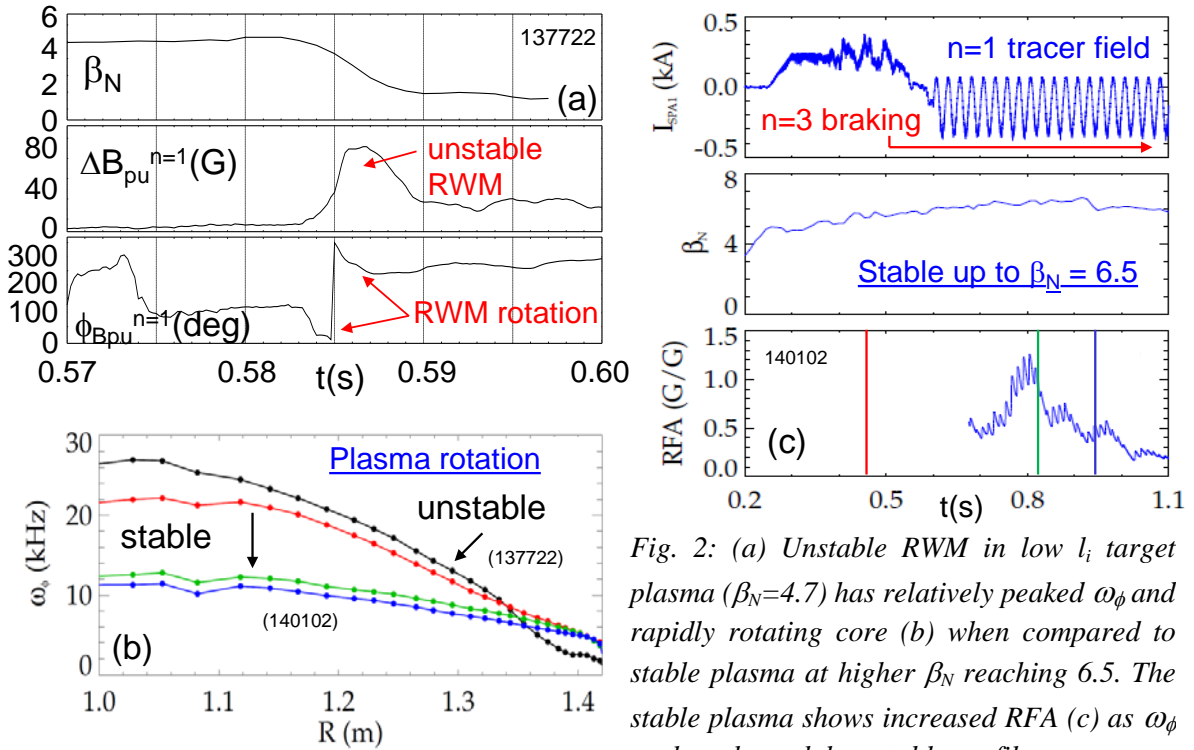


Fig. 2: (a) Unstable RWM in low l_i target plasma ($\beta_N=4.7$) has relatively peaked ω_ϕ and rapidly rotating core (b) when compared to stable plasma at higher β_N reaching 6.5. The stable plasma shows increased RFA (c) as ω_ϕ evolves through less stable profiles.

l_i plasmas with varying plasma toroidal rotation profiles, ω_ϕ . The RWM unstable plasma at $\beta_N = 4.7$ has the highest core rotation, while stable long-pulse plasmas with less peaked ω_ϕ have exceeded $\beta_N = 6.5$. Active MHD spectroscopy [4] of the stable plasma (Fig. 2c) shows an increase in resonant field amplification (RFA) of an applied $n=1$ AC tracer field, indicating a closer approach to RWM marginal stability. Greater instability seen at lower β_N/l_i is consistent with decreased passive RWM stabilization at intermediate plasma rotation levels caused by the rotation profile falling between stabilizing ion precession drift and bounce resonances. [5-7] Fig. 3 shows MISK stability code [5] calculations for a low l_i plasma experimentally reaching the $n=1$ RWM instability point. The marginally stable experimental

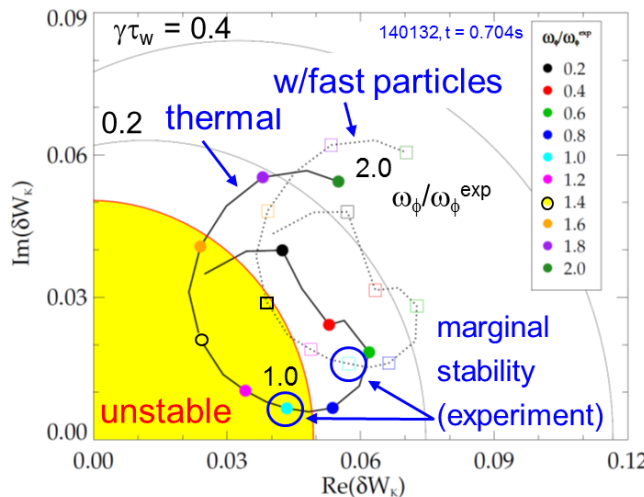


Fig. 3: MISK stability code calculations for a self-similar variation of ω_ϕ in a low l_i experimental plasma reaching RWM instability. Curves indicate calculations with/without the influence of isotropic fast particles.

additional modifications to the kinetic stabilization physics are underway to further improve this already close agreement between experiment and theory. [7]

In experiments using both poloidal (23) and radial field (24) RWM sensor arrays for feedback, the proportional gain and relative phase between the measured mode phase and applied control field phase were varied for each array. Modelled feedback evolution agrees with experiment for radial sensor variations (Fig. 4), and also shows the optimal gain is still a factor of 2.5 greater than the present value. In contrast, the experimentally optimal feedback phase for the poloidal sensors does not agree with theory (difference up to 90 degrees). Variations of plasma-induced mode helicity are being investigated as a potential cause.

The second approach for improved RWM stabilization is a newly-implemented RWM state-space controller using a state derivative feedback algorithm [8], and incorporating

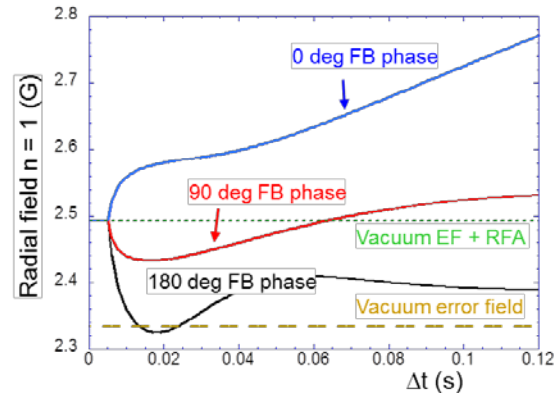
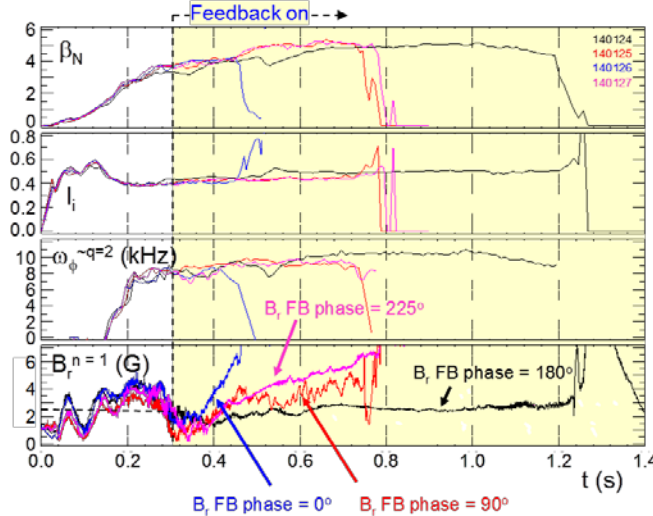


Fig. 4: RWM B_R sensor feedback phase variation with combined radial/poloidal field sensor feedback (a) experiment, (b) theory.

equilibrium points are indicated. Variation to either lower or higher ω_ϕ moves the plasma into stable regions. As is physically expected, considering thermal particles alone theoretically underestimates stability, and considering an isotropic fast particle distribution overestimates stability. Although the difference between theory and experiment is small ($\Delta\gamma\tau_w \sim 0.1$, where γ is the mode growth rate, and τ_w is the wall current decay time),

currents due to the RWM unstable eigenfunction and those induced in nearby 3D conducting

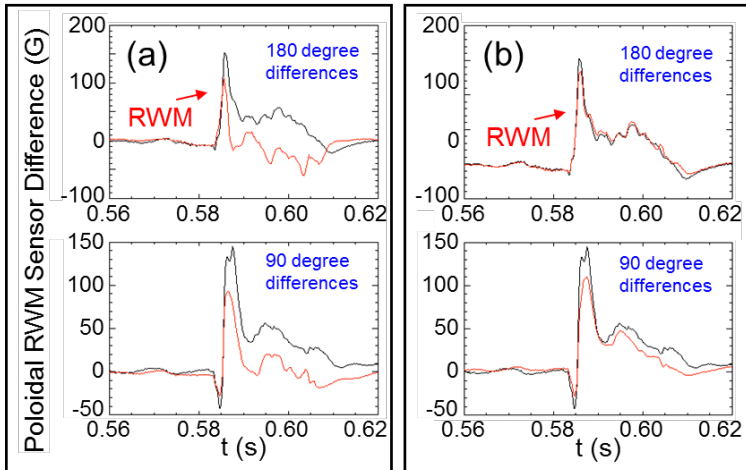


Fig. 5: Comparison of RWM B_p sensor difference measurements in an open-loop comparison of RWM state space control using (a) 2 states, and (b) 7 states.

sufficient 3D conducting structure current detail to match experimental sensors with greater fidelity during RWM activity (Fig. 5). This controller was used for RWM stabilization producing long-pulse plasmas (limited by coil heating constraints) (Fig. 6) reaching near maximum values of $\beta_N/l_i = 13.4$ (Fig. 1).

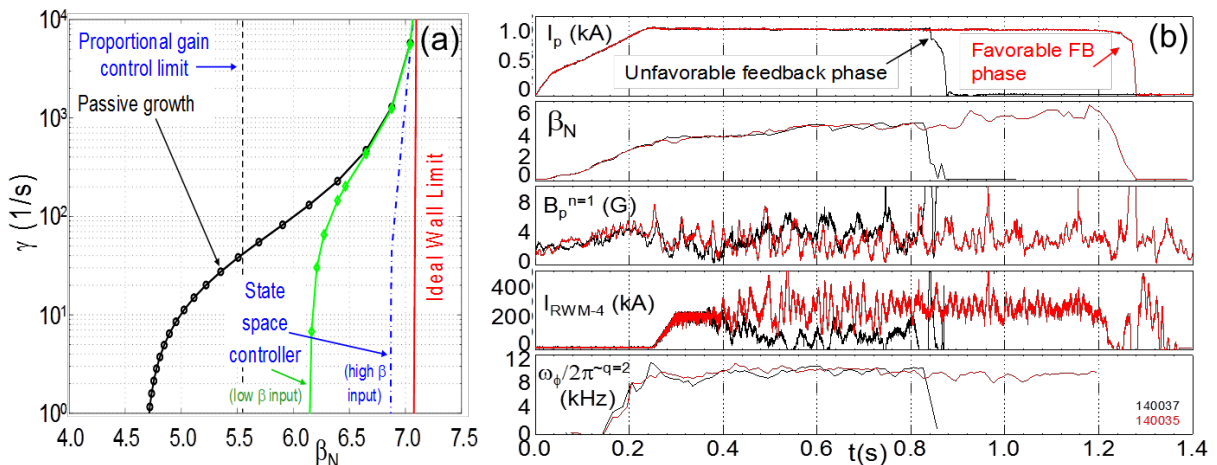


Fig. 6: (a) theoretical performance of RWM state space controller (at zero plasma rotation); (b) high β_N long-pulse plasma utilizing RWM state derivative feedback control.

*Supported by US DOE Contracts DE-FG02-99ER54524 and DE-AC02-09CH11466.

- [1] Y.-K. M. Peng, P.J. Fogarty, T.W. Burgess, *et al.*, Plasma Phys. Controll. Fusion **47** (2005) B263.
- [2] J.E. Menard, L. Bromberg, T. Brown, *et al.*, 23rd IAEA Conference, Daejeon, Korea 2010, paper FTP/2-2.
- [3] S.A. Sabbagh, A.C. Sontag, J.M. Bialek, *et al.*, Nucl. Fusion **46** (2006) 635.
- [4] H. Reimerdes, Chu MS, Garofalo AM, *et al.*, Phys. Rev. Lett. **93** (2004) 135002.
- [5] J.W. Berkery, S.A. Sabbagh, R. Betti, *et al.*, Phys. Rev. Lett. **104** (2010) 035003.
- [6] S.A. Sabbagh, J.W. Berkery, R.E. Bell, *et al.*, Nucl. Fusion **50** (2010) 025020.
- [7] J.W. Berkery, S.A. Sabbagh, R. Betti, *et al.*, (this conference) paper P1.078.
- [8] T.H.S. Abdelaziz and M. Valasek, Proc 16th IFAC World Congress, Prague (2005).
- [9] O. Katsuro-Hopkins, J.M. Bialek, D.A. Maurer, *et al.*, Nucl. Fusion **47** (2007) 1157.